

Average kinetic energy density of Cooper pairs above T_c in $\text{YBa}_2\text{Cu}_3\text{O}_{7-x}$, $\text{Bi}_2\text{Sr}_2\text{CaCu}_2\text{O}_{8+\delta}$ and Nb

S. Salem-Sugui, Jr.,¹ Mauro M. Doria,^{1,2} A. D. Alvarenga,³ V. N. Vieira,⁴ P. F. Farinas,¹ and J. P. Sinnecker¹

¹*Instituto de Física, Universidade Federal do Rio de Janeiro, 21941-972 Rio de Janeiro, Rio de Janeiro, Brazil*

²*Departement Fysica, Universiteit Antwerpen, Groenenborgerlaan 171, B-2020 Antwerpen, Belgium*

³*Instituto Nacional de Metrologia Normalização e Qualidade Industrial, 25250-020 Duque de Caxias, Rio de Janeiro, Brazil*

⁴*Departamento de Física, Universidade Federal de Pelotas, 96010-900 Pelotas, Rio Grande do Sul, Brazil*

(Received 13 August 2007; published 1 October 2007)

We have obtained isofield curves for the square root of the average kinetic energy density of the superconducting state for three single crystals of underdoped $\text{YBa}_2\text{Cu}_3\text{O}_{7-x}$, an optimally doped single crystal of $\text{Bi}_2\text{Sr}_2\text{CaCu}_2\text{O}_{8+\delta}$, and Nb. These curves, determined from isofield magnetization versus temperature measurements and the virial theorem of superconductivity, probe the order parameter amplitude near the upper critical field. The striking differences between the Nb and the high- T_c curves clearly indicate for the latter cases the presence of a unique superconducting condensate below and above T_c .

DOI: 10.1103/PhysRevB.76.132502

PACS number(s): 74.25.Bt, 74.25.Ha, 74.62.-c, 74.72.Bk

A considerable amount of evidence points toward the existence of superconductivity above the superconducting transition, T_c . Nernst coefficient measurements done in different compounds^{1,2} and also torque magnetometry in $\text{Bi}_2\text{Sr}_2\text{CaCu}_2\text{O}_{8+\delta}$ ($\text{Bi}2212$)¹ indicate a state with nonzero amplitude and phase incoherence,^{1,3} suggestive of a three-dimensional Kosterlitz-Thouless scenario inside the pseudogap region.^{1,4,5} According to the BCS theory, the electronic state acquires kinetic energy⁶ upon condensation, and for the high- T_c compounds, infrared and reflectivity measurements show a large transfer of spectral weight to the superfluid condensate,^{6,7} supportive of an in-plane kinetic energy driven mechanism. This kinetic energy gain holds for the overdoped $\text{Bi}2212$ compound but not for the optimally doped and the underdoped compounds,⁸ where the kinetic energy is, in fact, a loss. Thus, the kinetic energy is a relevant tool to sort the distinct proposals for the normal state and their consequent pairing mechanisms.^{7,8} Despite that, the literature lacks experimental information about the kinetic energy of the condensate in the presence of an applied field K , although a method to determine it has been proposed a few years ago.⁹ In this Brief Report, we show that this method is a tool to obtain information about the condensate above T_c . For instance, K provides information on the amplitude of the order parameter near T_c , a quantity of first importance to understand the nature of the superconducting state below and above T_c . There are several reports of a pseudogap that extends superconductivity above T_c for the high- T_c compounds,^{5,10-12} and they basically split into two views,¹³ either as directly related to the superconducting state or as a competing independent effect. The present results clearly support the first view although we do not directly probe the pseudogap in our study.

In this work, we obtain isofield curves of \sqrt{K} vs T and show that this quantity smoothly evolves from below to above T_c , without any abrupt change even in its first derivative with respect to the temperature, strongly suggestive of the existence of a unique condensate state below and above T_c for $\text{YBa}_2\text{Cu}_3\text{O}_{7-x}$ (YBaCuO) and for $\text{Bi}2212$. For comparison, we also study a low- T_c superconductor, e.g., ni-

bium (Nb), and find that our procedure is able to reproduce the standard BCS behavior. We chose to study \sqrt{K} because of its direct relation to the amplitude of the order parameter near T_c . For zero field, \sqrt{K} is proportional to the superconducting energy gap $\Delta(T)$ through the BCS expression $K \sim \Delta^2$.¹⁴

Average quantities can be determined in many-body physics by the virial theorem even in cases that knowledge about the interaction among particles is not complete. In classical systems, the virial theorem leads to remarkable estimates, e.g., the interior temperature of the Sun¹⁵ and an upper bound to the mass of a white dwarf star—the Chandrasekhar limit.¹⁶ Interestingly, the average kinetic energy of the condensate can be directly retrieved from the equilibrium magnetization M for a large κ type II superconductor, in the pinning free (reversible) regime.⁹ This connection is a direct consequence of the virial theorem:¹⁷

$$K = \left\langle \frac{\hbar^2}{2m} \left| \left(\nabla - \frac{2\pi i}{\Phi_0} \mathbf{A} \right) \psi \right|^2 \right\rangle = B|M|, \quad (1)$$

where ψ is the order parameter and B is the magnetic induction. The Abrikosov treatment¹⁸ of the Ginzburg-Landau theory gives that the average kinetic energy density of the condensate near the transition is

$$K = \frac{p^2}{2m} \langle |\psi|^2 \rangle = \frac{H[H_{c2}(T) - H]}{8\pi\kappa^2\beta_A}, \quad (2)$$

where $\langle \dots \rangle$ means spatial average, $p = \hbar\sqrt{2\pi H/\Phi_0}$, $H_{c2}(T) = \Phi_0/2\pi\xi(T)^2$, and $\beta_A \approx 1$ is the lattice constant. Thus, in this case too, \sqrt{K} is proportional to the average order parameter amplitude, and so, to the average superconducting energy gap. The general virial relation [Eq. (1)] applies throughout the mixed state and, consequently, reduces to Eq. (2) near the upper critical field, $H_{c2}(T)$. We find that the isofield \sqrt{K} vs T curves are well fitted by Eq. (2) for Nb with the expected coherence length temperature behavior [$\xi(T) \sim (T - T_c)^{-0.5}$], thus confirming a BCS gap behavior. However, this is not the case for the high- T_c compounds, whose average kinetic en-

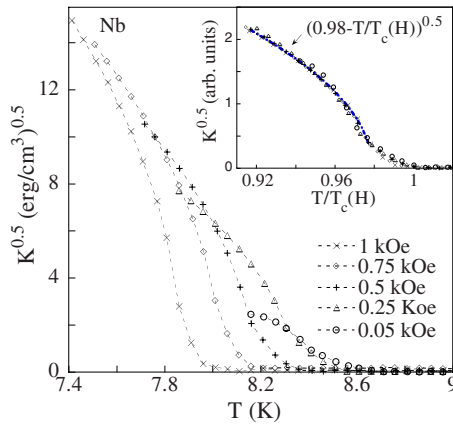


FIG. 1. (Color online) Selected isofield \sqrt{K} versus temperature curves are shown for Nb ($T_c=8.5$ K). The inset displays the collapse of these curves upon scaling and shows the fit agreement with the BCS-Abrikosov theory.

ergy density does not vanish at the BCS temperature $T_c(H) < T_c(0) = T_c$, but at some higher temperature, T^e , above T_c . Therefore, we show here that Eq. (1) is able to unveil the unusual properties of the gap in the presence of an applied field for the high- T_c compounds.

We measured three single crystals of $\text{YBa}_2\text{Cu}_3\text{O}_{7-x}$ ($T_c=93.2$ K for $x\sim 0.05$, $T_c=52$ K for $x=0.5$, and $T_c=41.5$ K for $x=0.6$), a single crystal of Bi2212 ($T_c=93$ K), and a Nb sample ($T_c=8.5$ K and Ginzburg-Landau parameter $\kappa=4$).⁹ The single crystals of YBaCuO and Bi2212 were grown at the Argonne National Laboratory¹⁹ and exhibit fully developed transitions with $\Delta T_c \approx 1-2$ K for YBaCuO samples and $\Delta T_c \approx 5$ K for Bi2212. The value of T_c for each sample is determined as the onset temperature of diamagnetism, above which magnetization values fall within the equipment sensitivity. Measurements of the isofield M vs T curves were done on (Quantum Design magnetic property measurement system and Lake-Shore) commercial magnetometers based on the superconducting quantum interference device. Experiments

were conducted for magnetic field values ranging from 0.05 to 6.0 kOe, always applied along the c axis direction of the crystals. Magnetization data, M vs T or M vs H curves, were always taken after cooling the sample below T_c in zero magnetic field (zero field colling). To determine the reversible (equilibrium) magnetization temperature range, we have also field cooled the samples from above to below T_c . The nonsuperconducting background was removed for each M vs T curve by fitting the magnetization in a temperature range well above T_c (~ 10 K for YBaCuO and ~ 20 K for Bi2212) to $M_{\text{back}} = A(H)$, where $A(H) = a - bH$ is a constant value for each field and a and b are constants determined for each sample. Above $H=1$ kOe, an additional term $C(H)/T$ had to be considered for deoxygenated YBaCuO, with $C(H)$ very small.²⁰ The determination of the average kinetic energy density requires that a few low temperature M vs H curves be measured in the Meissner region as a function of the applied field. These curves were obtained for all samples and yielded the geometric factor $d \equiv -H/M$ with a good resolution. Next, the geometrical factor is used to obtain the magnetic induction, $B \equiv H + dM$, which, in turn, is used to determine the \sqrt{K} vs T curves. Our Nb study is summarized in Fig. 1, which shows selected isofield \sqrt{K} vs T curves obtained from standard M vs T curves. We observe that the extrapolation of the isofield \sqrt{K} curves to the X axis (T axis) matches the $T_c(H)$ values obtained from the standard extrapolation of the magnetization curves to zero. Notice the collapse of all experimental different curves into a single one by a unique prescription, namely, by dividing the Y axis of each curve by a fixed number and rescaling T as $T/T_c(H)$. The resulting collapsed curve for Nb is shown in the inset of Fig. 1 and indeed shows the behavior $\sqrt{K} \sim (T - T_c)^{0.5}$ for T close to T_c , confirming that this quantity is proportional to the gap $\Delta(T)$.¹⁴ Hence, it carries information on the amplitude of the order parameter in the vicinity of T_c even for intermediated values of the applied magnetic field.

The \sqrt{K} curve leads to the average superconducting gap in the presence of an applied field, according to the BCS-Abrikosov theory. This assertion has far reaching conse-

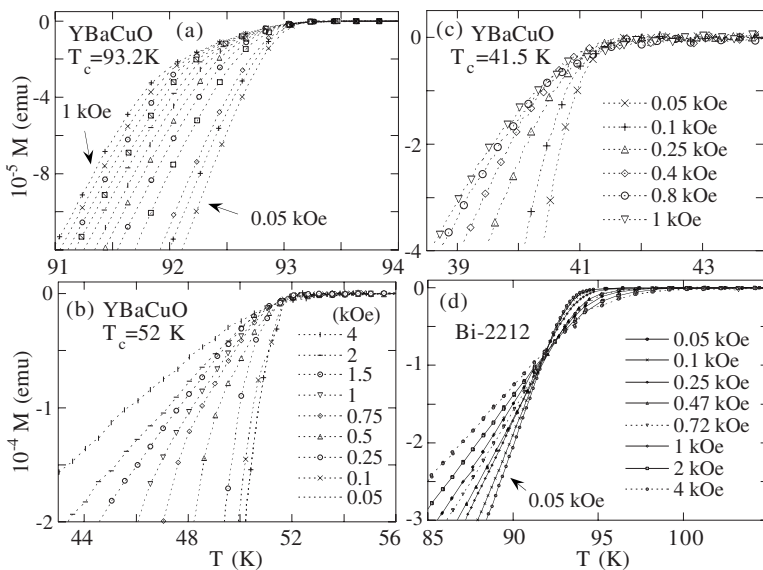


FIG. 2. Magnetization versus temperature curves are shown for several applied fields for YBaCuO and Bi2212 single crystals.

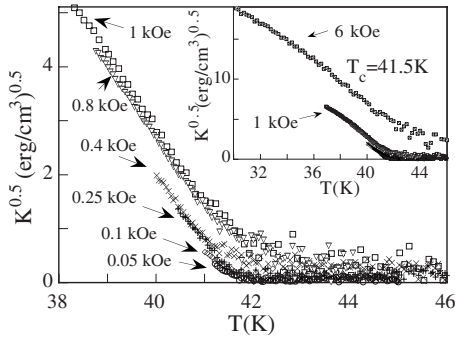


FIG. 3. Isofield \sqrt{K} versus temperature curves are shown for the YBaCuO compound. The inset displays an extra curve taken at a field above those shown in the main figure.

quences for the high- T_c superconductors, but we do not directly rely on it to do our data analysis, which is fully based on the general virial relation [Eq. (1)]. Figure 2 displays the M vs T reversible curves obtained for YBaCuO and Bi2212 samples. Our measurements reproduce standard and well known features below T_c , such as the nearly field independent crossing point^{21,22} for Bi2212. For YBaCuO,^{23,24} we also observe it for fields above 1.0 kOe. These crossing points are caused by thermal fluctuations on vortices and will not be discussed here. We reach our main results in Figs. 3–6, which show the \sqrt{K} vs T curves for the three doped YBaCuO and the Bi2212 compounds, respectively. They were obtained from the corresponding M vs T curves displayed in Fig. 2. The $d\sqrt{K}/dT < 0$ feature is common to all samples including Nb. However, a remarkable and striking difference exists between the high- T_c compounds and Nb. The temperature that \sqrt{K} extrapolates to zero, which indicates $T_c(H)$ for Nb and should decrease with H , instead, increases with H for the YBaCuO and Bi2212 compounds. The \sqrt{K} vs T YBaCuO and Bi2212 isofield curves enter the region above T_c smoothly, without any slope change. Then, owing to the present method, the state observed above T_c is found to be a continuous evolution of the condensate state below T_c . We find here that the isofield curves form a set of nonintersecting lines with roughly the same slope that eventually disappear inside a common background that surrounds the T axis. An increase in the applied field causes their shift to an upper region of the \sqrt{K} vs T diagram. The extrapolated

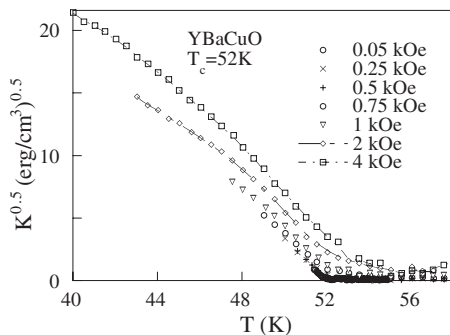


FIG. 4. Isofield \sqrt{K} versus temperature curves as obtained for the YBaCuO compound.

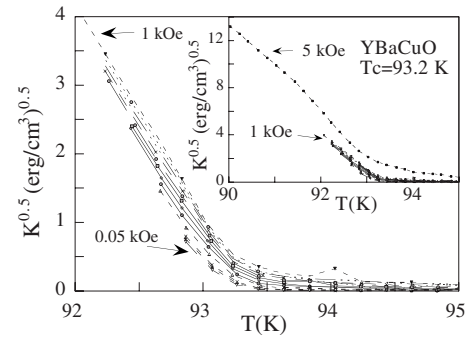


FIG. 5. Isofield \sqrt{K} versus temperature curves are shown for the YBaCuO compound. The inset displays an extra curve taken at a field above those shown in the main figure.

intercept of an isofield curve with the T axis defines a new temperature T^e , always found to be higher than T_c . Consider a $T > T_c$ vertical line in the \sqrt{K} vs T diagram. The intersect of the \sqrt{K} curves with this line defines a function $\sqrt{K}(H)$ that grows monotonically with H , in qualitative agreement with the $\sqrt{K} \sim \sqrt{H}$ prediction of Eq. (2). For temperatures above T^e , the background noise takes over the magnetization signal, rendering impossible any further analysis near the T axis. The nonintersecting feature of the \sqrt{K} vs T curves is a noticeable fact because it leads to the concept of the threshold field needed to produce a \sqrt{K} vs T curve above a given temperature T^e . For instance, the extrapolation of the Bi2212 curve $H=4.0$ kOe, shown in Fig. 6, toward zero occurs at $T^e \approx 99.3$ K. A \sqrt{K} curve that extrapolates to a higher temperature, $T'^e > T^e$, must be associated with a magnetic field larger than the threshold of 4.0 kOe.

It has been long known that critical fluctuations in the vicinity of T_c can produce effects on the normal state susceptibility for $T > T_c$,^{25,26} but they cannot explain our results because the Ginzburg criterion estimates a very small temperature window in the vicinity of T_c , where they are important: $G \sim \Delta T/T_c \approx 10^{-3}$.^{27,28} Even overestimating them, $\Delta T \approx 1$ K, keeps this window much below the 6 K shift above T_c found here for the $H=4.0$ kOe Bi2212 curve, for instance.

Theoretically, a pseudogap regime is a property of two-dimensional systems,^{29,30} and it is worth mentioning that a

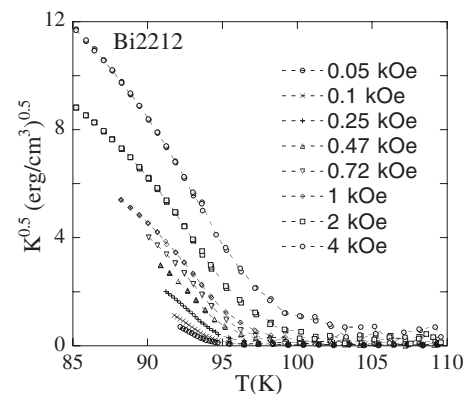


FIG. 6. Isofield \sqrt{K} versus temperature curves as obtained for the Bi2212 compound.

previous work,²⁰ performed on the same deoxygenated YBaCuO samples ($T_c=41.5$ and 52 K) used here, shows the existence of quasi-two-dimensional critical fluctuations in the region of T_c for low fields. We speculate that anisotropy plays an important role in the shift of the isofield \sqrt{K} vs T curves above T_c because doping effects on the pseudogap³⁰ are associated with dimensionality. Indeed, a direct inspection of Figs. 3–5 for YBaCuO and of Fig. 6 for Bi2212 show a correlation between the anisotropy ratio parameter γ and the relative temperature deviation above the critical temperature ($T^e - T_c$) of the \sqrt{K} vs T curves. These figures show that the Bi2212 [$\gamma \sim 200$ (Ref. 31)] has the most accentuated deviation, with $(T^e - T_c) \cong 6$ K for $H=4.0$ kOe, followed by the YBaCuO compounds in descending order of deviation:³² $T_c = 41.5$ K [$\gamma \sim 100$ and $(T^e - T_c) \cong 3.5$ K for $H=6.0$ kOe], $T_c = 52$ K [$\gamma \sim 65$ and $(T^e - T_c) \cong 2$ K for $H=4.0$ kOe], and $T_c = 93.2$ K [$\gamma \sim 8-9$ and $(T^e - T_c) \cong 0.3$ K for $H=5.0$ kOe]. We

stress that at T_c , \sqrt{K} grows continuously with field, and when the maximum is reached, this is the highest used field. Importantly, the latter clearly indicates a finite order parameter amplitude at T_c , and consequently, an upper critical field H_{c2} at T_c larger at least than the largest fields used here. Thus, our low field results are supportive of the high field scenario developed by Wang *et al.*^{1,3}

In summary, we have shown that the average kinetic energy density of the condensate exists above the critical temperature for the high- T_c but not for the low- T_c (Nb) compounds. It gives further evidence of a pseudogap, which has been directly measured by others^{5,10,11} in similar samples.

We thank Boyd Veal and D. G. Hinks from Argonne National Laboratory, who kindly provided the high- T_c single crystals. We thank CNPq, FAPERJ, and the Instituto do Milênio de Nanotecnologia for financial support.

-
- ¹Y. Wang, L. Li, M. J. Naughton, G. D. Gu, S. Uchida, and N. P. Ong, *Phys. Rev. Lett.* **95**, 247002 (2005).
- ²A. Pourret, H. Aubin, J. Lesueur, C. A. Marrache-Kikuchi, L. Berg, L. Dumoulin, and K. Behnia, *Nat. Phys.* **2**, 683 (2006).
- ³Y. Wang, L. Li, and N. P. Ong, *Phys. Rev. B* **73**, 024510 (2006).
- ⁴P. A. Lee, N. Nagaosa, and X.-G. Wen, *Rev. Mod. Phys.* **78**, 17 (2006).
- ⁵T. Timusk and B. Statt, *Rep. Prog. Phys.* **62**, 61 (1999).
- ⁶J. Corson, R. Mallozzi, J. Orenstein, J. N. Eckstein, and I. Bozovic, *Nature (London)* **398**, 221 (1999).
- ⁷A. F. Santander-Syro, R. P. S. M. Lobo, N. Bontemps, W. Lopera, D. Giratá, Z. Konstantinovic, Z. Z. Li, and H. Raffy, *Phys. Rev. B* **70**, 134504 (2004).
- ⁸G. Deutscher, A. F. Santander-Syro, and N. Bontemps, *Phys. Rev. B* **72**, 092504 (2005).
- ⁹M. M. Doria, S. Salem-Sugui, Jr., I. G. de Oliveira, L. Ghivelder, and E. H. Brandt, *Phys. Rev. B* **65**, 144509 (2002).
- ¹⁰L. D. Rotter, Z. Schlesinger, R. T. Collins, F. Holtzberg, C. Field, U. W. Welp, G. W. Crabtree, J. Z. Liu, Y. Fang, K. G. Vandervoort, and S. Fleshler, *Phys. Rev. Lett.* **67**, 2741 (1991).
- ¹¹H. Ding, T. Yokoya, J. C. Campuzano, T. Takahashi, M. Randeria, M. R. Norman, T. Mochiku, K. Kadowaki, and J. Giapintzakis, *Nature (London)* **382**, 51 (1996).
- ¹²M. Randeria, N. Trivedi, A. Moreo, and R. T. Scalettar, *Phys. Rev. Lett.* **69**, 2001 (1992).
- ¹³M. R. Norman, D. Pines, and C. Kallin, *Adv. Phys.* **54**, 715 (2005).
- ¹⁴P. G. deGennes, *Superconductivity of Metals and Alloys* (Addison-Wesley, New York, 1989).
- ¹⁵C. Kittel, W. D. Knight, and M. A. Ruderman, *Mechanics, Berkeley Physics Course* (McGraw-Hill, New York, 1965).
- ¹⁶G. W. Collins, II, *The Virial Theorem in Stellar Astrophysics* (Pa-
- chart, Tucson, 1977).
- ¹⁷M. M. Doria, J. E. Gubernatis, and D. Rainer, *Phys. Rev. B* **39**, 9573 (1989).
- ¹⁸A. Abrikosov, *Zh. Eksp. Teor. Fiz.* **32**, 1442 (1957) [*Sov. Phys. JETP* **5**, 1174 (1957)].
- ¹⁹B. W. Veal, A. P. Paulikas, H. You, H. Shi, Y. Fang, and J. W. Downey, *Phys. Rev. B* **42**, 6305 (1990).
- ²⁰S. Salem-Sugui, Jr., A. D. Alvarenga, V. N. Vieira, and O. F. Schilling, *Phys. Rev. B* **73**, 012509 (2006).
- ²¹L. N. Bulaevskii, M. Ledvij, and V. G. Kogan, *Phys. Rev. Lett.* **68**, 3773 (1992).
- ²²Z. Tesanovic, L. Xing, L. Bulaevskii, Q. Li, and M. Suenaga, *Phys. Rev. Lett.* **69**, 3563 (1992).
- ²³S. Salem-Sugui, Jr. and E. Z. da Silva, *Physica C* **235**, 1919 (1994).
- ²⁴B. Rosenstein, B. Y. Shapiro, R. Prozorov, A. Shaulov, and Y. Yeshurun, *Phys. Rev. B* **63**, 134501 (2001).
- ²⁵M. Tinkham, *Introduction to Superconductivity*, 2nd ed. (McGraw-Hill, New York, 1996).
- ²⁶Lu Li, Yayu Wang, M. J. Naughton, S. Ono, Yoichi Ando, and N. P. Ong, *Europhys. Lett.* **72**, 451 (2005).
- ²⁷R. A. Klemm, *Phys. Rev. B* **41**, 2073 (1990).
- ²⁸W. C. Lee, R. A. Klemm, and D. C. Johnston, *Phys. Rev. Lett.* **63**, 1012 (1989).
- ²⁹Y. M. Vilks and A. M. Tremblay, *J. Phys. I* **7**, 1309 (1997).
- ³⁰M. R. Norman, *Handbook of Magnetism and Advanced Magnetic Materials* (Wiley, New York, 2007).
- ³¹Y. Iye, I. Oguro, T. Tamegai, W. R. Datars, N. Motohira, and K. Kitazawa, *Physica C* **199**, 154 (1992).
- ³²T. R. Chien, W. R. Datars, B. W. Veal, A. P. Paulikas, P. Kostic, Chun Gu, and Y. Jiang, *Physica C* **229**, 273 (1994).